frontiers in Marine Science

ORIGINAL RESEARCH
published: 21 August 2018
doi: 10.3389/fmars.2018.00291

Modeling the Influence of Eutrophication and Redox Conditions on Mercury Cycling at the Sediment-Water Interface in the Berre Lagoon

Svetlana Pakhomova[1,2,3]*, *Evgeniy Yakushev*[3,4], *Elizaveta Protsenko*[3,4], *Sylvain Rigaud*[5], *Daniel Cossa*[6], *Joel Knoery*[7], *Raoul-Marie Couture*[8], *Olivier Radakovitch*[9,10], *Shamil Yakubov*[11], *Dominika Krzeminska*[12] and *Alice Newton*[1,13]

[1] Department for Environmental Impacts and Sustainability (IMPACT), Norwegian Institute for Air Research, Kjeller, Norway, [2] Department of Chemistry, Faculty of Natural Sciences, Norwegian University of Science and Technology, Trondheim, Norway, [3] Laboratory of Biohydrochemistry, P.P. Shirshov Institute of Oceanology RAS, Moscow, Russia, [4] Section of Oceanography and Biogeochemistry, Norwegian Institute for Water Research, Oslo, Norway, [5] Université de Nîmes, EA 7352 CHROME, Nîmes, France, [6] ISTerre, Université Grenoble Alpes, Grenoble, France, [7] IFREMER Département, RBE/BE, Nantes, France, [8] Département de Chimie, Université Laval, Québec, QC, Canada, [9] Aix-Marseille Université, CNRS, IRD, Collège de France, CEREGE, Aix-en-Provence, France, [10] Institut de Radioprotection et de Sûreté Nucléaire, PSE-ENV/SRTE/LRTA, Saint-Paul-Lez-Durance, France, [11] Institute of Coastal Research, Helmholtz-Zentrum Geesthacht, Geesthacht, Germany, [12] Norwegian Institute of Bioeconomy Research, Ås, Norway, [13] DCTMA-Department of Earth, Environmental and Marine Sciences, CIMA-Centre for Marine and Environmental Research, University of Algarve, Faro, Portugal

OPEN ACCESS

Edited by:
Selvaraj Kandasamy, Xiamen University, China

Reviewed by:
Armstrong-Altrin John S., Universidad Nacional Autónoma de México, Mexico
Rathinam Arthur James, Bharathidasan University, India

***Correspondence:**
Svetlana Pakhomova
s-pakhomova@yandex.ru

Specialty section:
This article was submitted to Marine Biogeochemistry, a section of the journal Frontiers in Marine Science

Received: *01 March 2018*
Accepted: *30 July 2018*
Published: *21 August 2018*

Citation:
Pakhomova S, Yakushev E, Protsenko E, Rigaud S, Cossa D, Knoery J, Couture R-M, Radakovitch O, Yakubov S, Krzeminska D and Newton A (2018) Modeling the Influence of Eutrophication and Redox Conditions on Mercury Cycling at the Sediment-Water Interface in the Berre Lagoon. Front. Mar. Sci. 5:291. doi: 10.3389/fmars.2018.00291

This study presents a specifically designed Mercury module in a coupled benthic-pelagic reactive-transport model - Bottom RedOx Model (BROM) that allows to study mercury (Hg) biogeochemistry under different conditions. This module considers the transformation of elemental mercury (Hg(0)), divalent mercury (Hg(II)) and methylmercury (MeHg). The behavior of mercury species in the model is interconnected with changes of oxygen, hydrogen sulfide, iron oxides, organic matter, and biota. We simulated the transformation and transport of Hg species in the water column and upper sediment layer under five different scenarios, combining various levels of oxygenation and trophic state in the Berre lagoon, a shallow eutrophic lagoon of the French Mediterranean coast subjected to seasonal anoxia. The first scenario represents the conditions in the lagoon that are compared with experimental data. The four other scenarios were produced by varying the biological productivity, using low and high nutrient (N and P) concentrations, and by varying the redox conditions using different intensity of vertical mixing in the water column. The results of the simulation show that both oxidized and reduced sediments can accumulate Hg, but any shifts in redox conditions in bottom water and upper sediment layer lead to the release of Hg species into the water column. Eutrophication and/or restricted vertical mixing lead to reducing conditions and intensify MeHg formation in the sediment with periodic release to the water column. Oxygenation of an anoxic water body can lead to the appearance of Hg species in the water column and uptake by organisms, whereby Hg may enter into the food web. The comparison of studied

scenarios shows that a well-oxygenated eutrophic system favors the conditions for Hg species bioaccumulation with a potential adverse effect on the ecosystem. The research is relevant to the UN Minimata convention, EU policies on water, environmental quality standards and Mercury in particular.

Keywords: mercury, methylmercury, biogeochemical modeling, anoxia, eutrophication, lagoon, BROM

INTRODUCTION

Mercury (Hg) is a global and ubiquitous metal that, while naturally occurring, has broad uses in everyday objects and is released to the atmosphere, soil and water from a variety of sources, (United Nations, 2017). It is a priority hazardous substance, (EC, 2000, 2008, 2017), of global concern, (United Nations, 2017), due to the magnitude of the anthropogenic emissions, long-range atmospheric transport from source regions, deposition on land and aquatic ecosystems as well as accumulation and bio-magnification within the food webs (Fitzgerald et al., 2007; Driscoll et al., 2013).

The chemistry of Hg in the aquatic environment is complex, involving many photochemical, thermochemical and biochemical reactions, making it difficult to predict its behavior and fate in the natural environments. Depending on physical, chemical and biological conditions, Hg compounds in aquatic systems can be interconverted, released from the sediment to the water, taken up by biota, released to the atmosphere, or transported with particulate matter to other uncontaminated locations. Hg is present in the environment in elemental form (Hg (0)), and in various divalent forms (Hg(II)), including inorganic and organic compounds. Hg transformations involve two, main, reversible reactions (Fitzgerald et al., 2007): redox reactions converting Hg(0) to Hg(II) and involving air-water exchange of the volatile Hg(0) followed by its oxidation; and methylation-demethylation reactions converting inorganic Hg (II) to methylated species that are much more toxic to aquatic organisms than inorganic forms of Hg (Fitzgerald and Clarkson, 1991). The major organic form of Hg is methylmercury (MeHg), a neurotoxin that accumulates in biota and is biomagnified in aquatic food-webs (Fitzgerald and Clarkson, 1991). As all these processes are redox dependent, Hg speciation, partition and mobility in aquatic water and sediments depends on redox conditions.

The Hg cycle is coupled with the dynamic of organic matter (OM) (Chakraborty et al., 2015), Fe and sulfide cycles (Jeong et al., 2010), and depends on the microbiological context (Cossa et al., 2014; Bigham et al., 2016). The Sediment Water Interface (SWI) is a zone of active redox processes and a key zone for important Hg transformation and transfers. The SWI is the boundary between bed sediment and the overlying water, a zone going from the deepest centimeters of the water column to the first few centimeters of the sediment. Anthropogenic activities and emissions perturb the natural Hg cycle due to the extensive industrial use of Hg and emissions from fossil fuel combustion. These pressures result in serious contamination of surface waters, biota and sediments (Liu et al., 2012; Driscoll et al., 2013). Sediments are often the main Hg reservoir in aquatic systems but can also act as a potential source of Hg (Covelli et al., 1999) and may pose a risk to aquatic life for many years (Kudo, 1992, O'Higgins et al., 2014).

Field measurements are often too limited to capture the necessary information to understand the Hg cycle processes at the SWI and to predict the fate of Hg in the aquatic environment. These Hg cycle processes include rapid, biogeochemical dynamic processes, Hg processes of speciation transformation. Environmental modeling can be used to complement the field observation and to get better understanding of the highly dynamic behavior and fate of Hg in aquatic ecosystems.

Hg modeling tools have been developed for several aquatic environments: lakes, freshwaters, estuarine, and marine waters (Wang et al., 2004; Knightes, 2008; Massoudieh et al., 2010; Canu et al., 2012). Standard Hg modeling applications generally represent the Hg cycle in the dissolved and in one or more different phases (silt, clay, detritus, plankton, and organic carbon), which is generally calculated using partition coefficients. The transformation processes are generally of first-order and in some cases temperature-dependent. Bioaccumulation processes in the trophic chain are often not considered. In some cases, they are simulated via bioaccumulation factors (BAFs) or using fish energetics (Barber et al., 1991). Processes leading to the change in Hg speciation are generally ignored and Hg compounds are lumped into three groups: Hg(0), Hg(II), and MeHg. Hg(II) generally is a sum of all dissolved inorganic and organic species.

The present study is a new version of the 1D benthic-pelagic coupled biogeochemical model, BROM (Yakushev et al., 2017) supplemented by a Hg module specifically developed for the study (**Figure 1**). Transformations of variables are considered both in the water column and in the upper sediment layer, as well as exchange with the atmosphere for gases [e.g., O_2, CO_2, Hg(0)]. The Hg module that has been developed considers Hg species transformations interconnected with other chemical compounds involved in the Hg cycle: O_2, H_2S, Fe, dissolved and particulate OM and biota. Simulation of redox-dependent changes is a convenient way of studying Hg fate under variable redox conditions.

The Etang de Berre lagoon, (France), is a Mediterranean coastal lagoon with brackish waters (salinity is ranging between S = 15–30) and an average depth of 6 m (maximum depth ∼9.5 m, **Figure 2**). The sediments have accumulated large amounts of pollutants due to past industrialization, including Hg species that reach up to 3 $\mu g\ g^{-1}$ in the surface sediment (Rigaud et al., 2011). In addition, redox conditions in the water column are very variable over time, due to the occurrence of seasonal hypoxia, mainly driven by both high productivity due to large nutrient concentrations (i.e., eutrophication) and reduced water mixing because of the haline stratification of the water column. Hypoxia events are very common in summer, leading to frequent anoxia and sulphidic conditions in the bottom

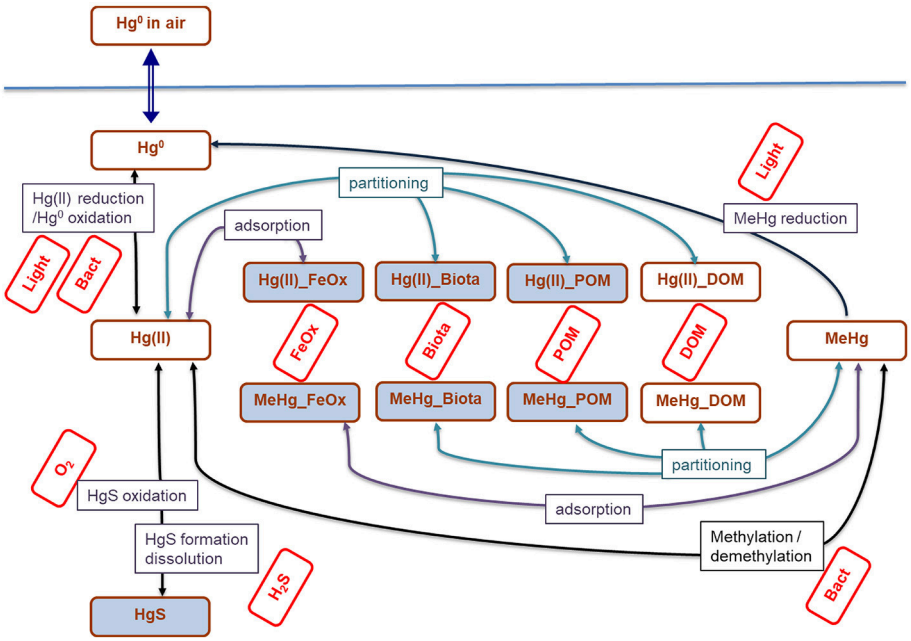

FIGURE 1 | Mercury transformations in aquatic ecosystems parametrized in the brom_hg module. Brown rectangles correspond to the state variables in the brom_hg module, red rectangles correspond to the state variables of BROM (Yakushev et al., 2017), whose concentrations are used in calculations of Hg transformations. Uni-directional arrows reflect the processes considered in the model and the bi-directional arrow represent air-water fluxes. Open brom_hg rectangles represent dissolved species and shaded ones represent particulate species. Hg enters the system via exchange with the atmosphere; all other processes occur both in the pelagic and benthic parts of the model.

water column. Both sediment contamination and hypoxia events lead to a strong degradation of the benthic ecosystems. The environmental managers of the Berre lagoon attempt to limit these eutrophication and hypoxia events. They therefore need a better understanding of the risks associated with the remobilization of contaminants accumulated in the sediment. They also need knowledge of the biogeochemical dynamics of Hg species at the SWI under the current redox/eutrophication conditions and under the potential future changes.

In this study, we use an updated version of BROM to simulate seasonal dynamics of redox conditions in the bottom water of the Berre lagoon. The main goal is to capture the effect of redox conditions and trophic state on Hg species mobilization under different conditions. Results will be used to predict the fate of Hg in the Berre lagoon sediment in the current situation and in the future under expected higher redox conditions and lower trophic state.

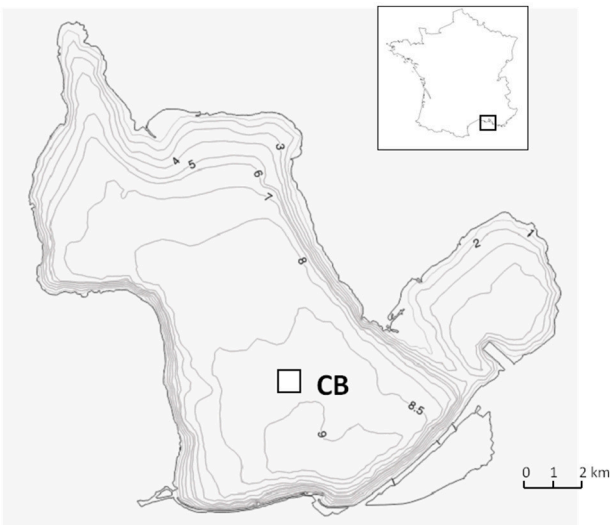

FIGURE 2 | Map of the Berre lagoon and sampling site.

DATA AND METHODS

Modeling

General Description of BROM Model

This work is based on the fully coupled benthic-pelagic biogeochemical model BROM (Bottom RedOx Model, Yakushev et al., 2017). BROM consists of a 1-dimentional vertical transport module (BROM-transport) and a biogeochemical module (BROM-biogeochemistry) coupled through the Framework for Aquatic Biogeochemistry Model (FABM) Bruggeman and Bolding, 2014). The model considers interconnected transformations of N, P, Si, C, O, S, Mn, and Fe species in the water column, bottom boundary layer (BBL) and upper sediment. In this new version of the model, BROM-biogeochemistry is divided on 20 different modules

that can be used independently (*brom_bio, brom_nitrogen, brom_fe etc.*). BROM simulates a simple ecosystem composed of autotrophic (Phy) and heterotrophic (Het) organisms as well as four types of bacteria (aerobic heterotrophic and autotrophic bacteria, and anaerobic heterotrophic and autotrophic bacteria). OM dynamics include parameterizations of both OM production, via photosynthesis, chemosynthesis, and decay; via oxic mineralization, denitrification, metal reduction, sulfate reduction, and methanogenesis, with a decreasing rate of OM decay in this sequence. The detailed description of the model can be found in Yakushev et al. (2017). The source code and description of the new version are available at https://github.com/BottomRedoxModel.

Mercury Cycle Parametrization

The mercury module (*brom_hg*) considers the transformation of different species of Hg in line with changes of other BROM variables (**Figure 1**). We parametrized reactions of Hg(0), Hg(II) and MeHg (oxidation/reduction, (de)methylation, formation/dissolution of HgS) as well as Hg adsorption on Fe oxides (Fe3) and Hg partitioning with particulate and dissolved organic matter (POM and DOM), as well as bioaccumulation by biota (**Figure 1**, **Tables 1**, **2**). Adsorption on Fe oxides was parametrized according to Katsev et al. (2006). Partitioning was parametrized as described by Mackay (2001). Bioaccumulation by biota includes autotrophs, heterotrophs and all types of bacteria.

Boundary Conditions

The model domain spans from the sea surface (upper boundary) down to 10 cm depth in the sediment (lower boundary). At the upper boundary, the fluxes of O_2, CO_2, NO_3^-, PO_4^{3-}, Si, Hg(0) and Fe and Mn oxides were defined. Fluxes for all other modeled chemical constituents were set to zero. For CO_2 and Hg(0), the surface fluxes were calculated proportional to the difference of their concentrations in the surface water and constant atmospheric concentrations of CO_2 (380 ppmv) and Hg(0) (3 ng/m^3). Exchange of O_2 was parameterized as a function of the O_2 saturation in the surface water. Inputs of PO_4^{3-}, NO_3^-, Fe, and Mn from atmospheric deposition and rivers were taken into account by forcing concentrations at the water surface. There is a natural, seasonal variability of inputs of PO_4^{3-} and NO_3^-. The maximum concentrations are in the winter-spring period (up to 1.6 and 15 μM for PO_4^{3-} and NO_3^-). The minimum concentrations (down to undetectable) are in the summer period. A constant surface concentration of 5×10^{-4} μM was prescribed for Fe(III) and Mn(IV). The concentrations at the lower boundary result from the processes that occurred in the water column, BBL and upper sediment. Therefore, the model biogeochemistry is predominantly forced by the upper boundary conditions.

Hydro-Physics

BROM-transport requires forcing for temperature, salinity, and turbulent vertical diffusivity at all depths in the water column and for each day of the simulation. For the Berre lagoon application, we used the output from the TELEMAC model, (Jeliazovski et al., 2015). The vertical diffusion coefficient k_z was calculated based on vertical density distributions, following approach by Gargett (1984) such that k_z:

$$K_z = a_0 N^{-q}$$

where $N = \sqrt{-\frac{g}{\rho}\frac{\partial \rho}{\partial z}}$, is the buoyancy frequency and a_0, and q are empirical coefficients.

For the specific case of the Berre Lagoon, values of those coefficients were set to 0.5×10^{-6} and 0.5, respectively. For the BBL, k_z was assumed to be constant with value 0.5×10^{-6} m^{2}s^{-1}.

In the sediments, k_z was parameterized as a sum of the pore water molecular diffusion coefficient $K_{z\_mol} = 1 \times 10^{-11}$ m^{2}s^{-1} and the bio-irrigation and sediment biomixing coefficient with a maximum value 0.1×10^{-11} m^{2}s^{-1} in the upper 5 mm of the sediments and exponentially decreasing deeper, as described in Yakushev et al. (2017). Bioturbation occurs in cases where oxygen concentrations in the bottom water are higher than 5 μM.

Scenarios

We first simulated the "baseline variability" (scenario S1) based on the present state of the lagoon. S1 reproduces the eutrophied system with seasonal anoxia and H_2S in the bottom water (BW). This simulation was compared with the data from the 2009 and 2010 field surveys (see section below).

The three following scenarios (S2–S4) were simulated in order to understand the effects of redox conditions on the biogeochemical cycle of mercury for eutrophied and non-eutrophied systems (**Table 3**):

S2. The lagoon with eutrophication and perennially oxygenated water-column. BW is oxygenated throughout the year due to high vertical mixing and in spite of the high concentrations of nutrients in the surface water.

S3. The lagoon without eutrophication but with the occurrence of hypoxic, yet non-sulphidic conditions. BW is hypoxic throughout the year due to reasonably low concentrations of nutrients in the surface water but there is less vertical mixing.

S4. The lagoon without eutrophication and anoxic conditions. BW is oxygenated throughout the year due to reasonably low values of nutrients in the surface water and present vertical mixing.

For the scenarios S1-S4, the calculations were started from the same initial conditions: zero concentrations for all the model variables in the water and sediments. However, the boundary conditions were different: greater or smaller nutrient concentrations in the water surface and different mixing intensity of the water column (**Table 3**). The seasonal dynamics of biogeochemical variables became stable after about 20 years of calculations (spin-up period).

Finally, we simulated the scenario of an artificial, intensive, vertical mixing, applied to oxygenate the Berre lagoon bottom water (S5). Such mixing may correspond to a possible management solution by using aeration system (i.e., propeller,

TABLE 1 | Parameters names, notations, values and units of the coefficients used in the model.

Reactions	Constants		
	Name, unit	**Value direct/reverse**	**References**
Hg(0) ↔ Hg(II) (photochemical reaction)	K_{ox}/K_{red}, d^{-1}	5.89/0.05	(Knightes, 2008) this work
Hg(0) ↔ Hg(II) (microbiological reaction)	K_{ox}/K_{red}, d^{-1}	1.44/0.005	(Knightes, 2008) this work
Hg(II) ↔ MeHg (microbiological reaction)	$K_{metil}/K_{demetil}$, d^{-1}	0.8/0.5	(Knightes, 2008) this work
MeHg → Hg(0) (photochemical reaction)	K_{red}, d^{-1}	0.002	Knightes, 2008
Hg(II) ↔ HgS	K_{sp}, M^2 K_{form}/K_{diss}, d^{-1}	10^{-6}, $1 \times 10^{-8}/1 \times 10^{-13}$	(Waples et al., 2005); this work
ADSORPTION/COMPLEXATION			
Hg(II) and MeHg on DOM/POM	log K_d, L/kg	5.0	Allison and Allison, 2005
Hg(II) and MeHg on Fe_2O_3	log K_d, L/kg	5.0	(Allison and Allison, 2005; Katsev et al., 2006); this work
BIOACCUMULATION			
Hg(II) and MeHg	log K_d, L/kg	5.0	Bruggeman and Bolding, 2014

TABLE 2 | Variables used in *brom_hg*.

Variable	Description	Variable	Description
Hg0	zero valent Hg, dissolved	MeHg	free MeHg, dissolved
Hg2	free bivalent Hg, dissolved	MeHg_DOM	MeHg bounded with DOM, dissolved
Hg2_DOM	bivalent Hg bounded with DOM, dissolved	MeHg_POM	MeHg bounded with POM, particulate
Hg2_POM	bivalent Hg bounded with POM, particulate	MeHg_Fe3	MeHg bounded with Fe oxides, particulate
Hg2_Fe3	bivalent Hg bounded with Fe oxides, particulate	MeHg_biota	MeHg bounded with biota, particulate
Hg2_biota	bivalent Hg bounded with biota, particulate	MeHg_tot_diss	total MeHg, dissolved (MeHg + MeHg_DOM)
Hg2_tot_diss	total bivalent Hg, dissolved (Hg(II) + Hg(II)_DOM)	Hg_tot_diss	total dissolved Hg (Hg(0) + Hg(II)_tot_diss + MeHg_tot_diss)
HgS	Hg sulfide, particulate	%MeHg	percent ratio of MeHg (MeHg_tot_diss/Hg_tot_diss)

TABLE 3 | Parameters of studied scenarios (S1–S4) used in numerical experiments.

	Lower mixing ($k_z \sim 10^{-7}$ m^2/s)	**Present mixing ($k_z \sim 10^{-6}$ m^2/s)**	**Higher mixing ($k_z \sim 10^{-5}$ m^2/s)**
Present nutrient concentrations, $c(NO_3^-)max = 15\,\mu M$		Changeable redox conditions in BW, present state, S1	Oxic conditions in BW, S2
Lower nutrients concentrations, $c(NO_3^-)max = 2\,\mu M$	Hypoxia in BW, S3	Oxic conditions in BW, S4	

bubbler). In this S5 scenario, we first made 21 years of calculations, exactly analogous as for S1 (present nutrient concentrations and vertical mixing), to achieve the present biogeochemical state of the lagoon. We then increased vertical mixing ($k_z \sim 10^{-2}$ m^2/s) during the 22nd year. From the 23nd year, the initial vertical mixing ($k_z \sim 10^{-6}$ m^2/s) was used for the calculations and maintained constant over a 7 year period.

Observations

The data used were obtained in summer 2009 and summer 2010 in the southern part of the Central basin in the Berre Lagoon, where anoxic/hypoxic events occurred (site CB, Rigaud et al., 2013, **Figure 2**). Two contrasted redox situations in the bottom of the water column were encountered during the field campaigns: anoxic/sulphidic conditions ($O_2 < 0.2\,mg\,L^{-1}$; $\sum H_2S = 100\,\mu M$) prevailed in summer 2009; oxic conditions ($O_2 = 2.9\,mg\,L^{-1}$) prevailed in summer 2010. The dataset consisted of vertical profiles of physico-chemical parameters (salinity, pH, Eh) and of the concentrations of the main, dissolved, chemical species, (Fe, Mn, SO_4^{2-}, ΣH_2S, ΣPO_4, tCO_2, NH_4^+, ΣNO_3, DOC, Hg_{tot}, MeHg), obtained from 15 cm above SWI to a depth of 35 cm in the sediment. Details about sampling are given in Rigaud et al. (2013). In addition, the vertical distribution of dissolved chemical species in the benthic boundary layer was investigated using the SUSANE sampler, a high vertical resolution bottom water sampler. This device

was deployed twice during summer 2009 during anoxic/non sulphidic and anoxic/sulphidic conditions.

The total dissolved Hg (Hg_{tot}) concentrations were determined using cold-vapor atomic fluorescence spectrometry (CVFAS, Tekran). The accuracies were confirmed using the reference material ORMS-4 (NRCC) and were approximately 5%. The analysis of dissolved MeHg was performed using atomic fluorescence spectrophotometry following the protocol developed by Tseng et al. (1998). The details of the chemical analysis are given in Rigaud et al. (2013).

RESULTS AND DISCUSSION

Current Hg Biogeochemistry in the Lagoon (S1)

General Biogeochemical Processes

The modeled redox conditions at SWI in the Berre lagoon in the scenario S1 oscillates over the year (**Figure 3**), which is in agreement with the seasonal hypoxia-anoxia that is known to occur in the area, (Rigaud et al., 2013). The simulation is in agreement with the field measurements for concentration ranges, vertical distribution and seasonal dynamics of O_2, H_2S, pH, nutrients, alkalinity, DOM, dissolved reduced species of iron and manganese [see examples for O_2, H_2S, Mn(II), and Fe(II) in **Figure 4**]. The observed concentration of O_2 in the BW of the lagoon varied from about 20 μM to undetectable during the summer, which coincides with the modeled concentration of scenario S1. Measured concentrations of H_2S reached 150 μM in the BW and up to 300 μM in porewater that is also in agreement with the S1 results. The modeled dissolved Fe(II) and Mn(II) concentrations decrease in the porewaters and increase in BW during anoxia in summer period that coincides with the observations (**Figures 3**, **4**).

The model simulations demonstrate some fundamental features of SWI biogeochemistry in the lagoon that are described in Rigaud et al. (2013) and completed here (**Figure 3** for water column and upper sediment distributions and **Figure 5** for a zoom on the particulate composition at the SWI). Briefly, during the oxygenated winter period, the oxic/anoxic interface was positioned at several millimeters depth in the sediments (**Figures 3**, **4**). During the bloom period an intensive formation of OM in the water column and export to the surface sediment (**Figure 3**) results in O_2 consumption in the BBL in early spring (**Figure 3**). This induced the degradation of the accumulated POM at the SWI, with a slower rate for other oxidizing agents, NO_3^-, Mn(IV), Mn(III), Fe(III) and SO_4^{2-}. The reduction of Mn and Fe oxides in the upper millimeters of the sediments (**Figure 5**) induced fluxes of Mn and Fe to the water column (**Figure 3**) after the disappearance of oxygen at the SWI, in February. The hydrogen sulfide (H_2S), initially constrained in the porewaters, enters the water column (**Figure 3**) about a month later, once the reservoir of oxidizing agents has been consumed. High concentrations of H_2S in the water column last over the summer. Higher wind forcing and lower temperature lead to an abrupt increase of O_2 and disappearance of H_2S in the bottom water (**Figure 3**) from November, as well as the appearance of Mn(IV), Mn(III), and Fe(III) in the water column, and their accumulation at the sediment surface (**Figure 5**). During the winter, the oxic/anoxic interface is lowered to a deeper level in the sediments. The microbial community also changes over the year, shifting from heterotrophic and autotrophic aerobic bacteria to anaerobic heterotrophic bacteria (**Figure 3**), in response to the redox conditions. The modeled anaerobic heterotrophic bacteria (Bhan) correspond to sulfate reducing bacteria (SRB) because sulfate reduction is the most important process for anoxic OM mineralization. The described biogeochemical cycle recurs annually in relation to the seasonal cycle of production/degradation of the OM and hydro-climatic forcing within the lagoon.

Dynamics of the Hg Species

Simulated Hg and MeHg concentration profiles are in agreement with the field measurements (**Figure 4**) with the minimum Hg species concentrations in BW under oxic conditions and the maximum concentrations under anoxic conditions (**Figure 3**). According to the model, the fraction of the Hg_{tot} that is dissolved MeHg (MeHg/Hg_{tot} ratio) amounts up to 0.65 (65%) in porewater and up to 0.4 (40%) in the BW during anoxia events. This is also in agreement with measured data (Rigaud et al., 2013).

The concentration of Hg_{tot} is low in the water column, (0.5 pM or less, **Figure 3**), due to its adsorption on Fe oxy-hydroxides and POM at the SWI under oxic conditions in the BW and upper sediment layer (i.e., from November to February), as model results shows (Hg2_Fe3 and Hg2_POM, **Figure 5**). The continuous presence of H_2S resulted in the formation of insoluble HgS that is the main pool of Hg in the sediment (**Figure 5**). The deepest penetration of O_2 into the sediment in January leads to the oxidation of reduced sediment layer and decrease of HgS concentration there. Low concentrations of dissolved MeHg observed in the upper sediment layer are due to MeHg adsorption on Fe oxy-hydroxides at the SWI that prevents the release of MeHg to the water column. This corresponds to the period of maximum MeHg adsorbed on Fe oxy-hydroxides (MeHg_Fe3) (**Figure 5**). The upward migration of H_2S induced the release of the adsorbed Hg and MeHg species in the porewaters (from February) producing a short but intensive peak of Hg species content in the BW in March, due to the fast dissolution of Fe oxides at SWI in anoxic conditions (**Figures 3**, **5**). The further increase of H_2S concentration leads to the formation of insoluble HgS, resulting in a decrease in Hg species concentration both in the porewater and bottom water. Wind events give rise to rapid and episodic oxygenation. The occurrence of oxygen in the bottom water during the anoxia period, even at low ($O_2 < 10$ μM) concentrations, induces rapid H_2S disappearance (**Figure 3**) and a decrease of dissolved Hg and MeHg concentrations in the BW and at the sediment surface, when Hg and MeHg are adsorbed on newly formed Fe oxides at the SWI (**Figure 5**). After these oxygenation events, once reducing conditions are reestablished in the BW, a new peak of dissolved Hg species in the water column occurs, followed by HgS formation (**Figures 3**, **5**). Thus, the maximum concentrations of dissolved MeHg and Hg(II) at the SWI (up to 0.24 and 0.5 nM) occurred during the shift from oxic to anoxic conditions,

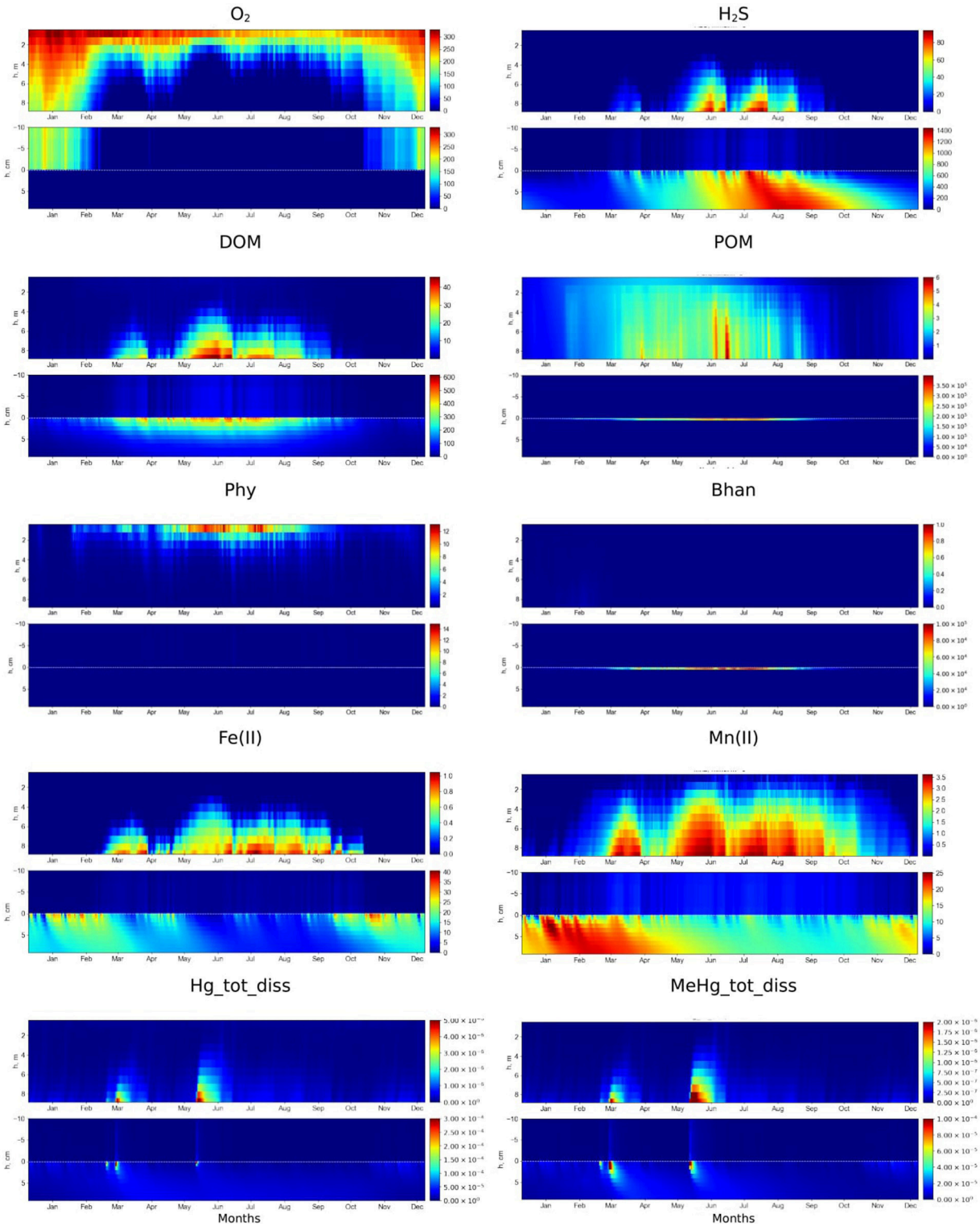

FIGURE 3 | Simulated seasonal dynamics of dissolved oxygen, hydrogen sulfide, DOM, POM, phytoplankton (Phy), anaerobic heterotrophic bacteria (Bhan), dissolved Fe(II), Mn(II), total dissolved Hg and MeHg (μM) in the water column and at the sediment-water interface (±10 cm) in the Berre lagoon according to scenario S1.

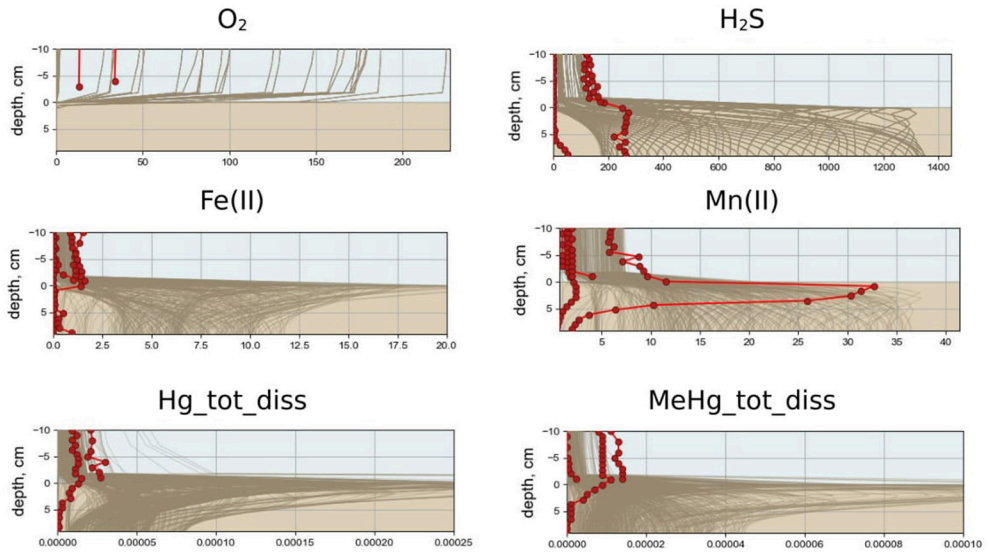

FIGURE 4 | Annual variability of simulated vertical distribution of dissolved oxygen, hydrogen sulfide, Fe(II), Mn(II), total dissolved Hg, and MeHg (μM) for scenario S1 (lines) and measured in summer 2009 and summer 2010 (dots) in the bottom water and at upper sediment layer in the Berre lagoon.

when accumulated Hg species are released from the oxide reservoir, and with the apparition of H_2S (**Figures 5**, **6**). The POM in the surface sediment during the reducing conditions accumulates Hg species at the SWI, but the POM is Hg and MeHg depleted deeper in the sediment (**Figure 5**). This indicates that the precipitation of HgS is a more efficient process than Hg species accumulation into OM. Under oxygenated conditions in the water column (from October), both Hg2_POM/MeHg_POM and Hg2_Fe3/MeHg_Fe3 increase in the surface sediment and no dissolved Hg appears in the upper sediment and BW (**Figures 3**, **5**, **6**). This indicates that the Hg species preferentially accumulate on Fe oxides, biota and freshly deposited OM. The maximum concentration of MeHg bioaccumulated on biota occurs at the SWI under oxic conditions, in periods of minimum content of dissolved MeHg in the BW and upper sediment.

We can use the model to make predictions because the results fit well with the experimental data. We are able to relate the Hg modeled dynamic to the SWI biogeochemistry in relation to redox variation. The main parameters influencing Hg cycling at the SWI are redox conditions in the BW/upper sediment layers and the Fe, S and OM cycles. We tested the response of the Hg cycle to the different combinations of these key environmental variables in the lagoon, under plausible scenarios of redox conditions in relation to variable oxygenation and eutrophication conditions.

Hg Biogeochemistry Under Different Conditions

Influence of the Redox Conditions in Eutrophied System (S1 vs. S2)

The summer formation of H_2S in the sediment is 5-10 times greater in a eutrophied system, with seasonal anoxia in the BW (S1), with respect to a well-oxygenated eutrophied system (S2), (**Figure 7**). The high concentration of O_2 in the BW throughout the year inhibits H_2S release to the BW in S2. The POM content in the upper sediment in S2 is a third of S1, because the degradation of OM is faster in the presence of O_2 than using other oxidizing agents (**Figure 5**). Fe oxy-hydroxides are present in the surface sediment throughout the year, with lower concentrations in the summer period (**Figure 5**). Fe oxy-hydroxides concentrations in the surface sediment are similar for S1 and S2 scenarios during the winter.

Dissolved Hg concentration in the water column and sediment is higher in S2 than in S1, because of the lower concentration of H_2S in the surface sediment and consequently less binding of Hg with sulfide in the sediment. HgS is not the main pool of Hg in S2 (**Figure 5**). Fe oxy-hydroxides and POM are the main sinks for Hg species in the presence of low concentration of H_2S in a eutrophied system, (**Figure 5**). The role of particulate OM is most important during the summer period (i.e., Hg2_POM>Hg2_Fe3) when Fe3 concentrations are lower (**Figure 5**).

Most of the MeHg that is formed in S2 is adsorbed on Fe oxy-hydroxides and POM at the SWI and therefore not released into the BW (**Figures 5**, **7**). High concentrations of MeHg (60 pM) appears at the SWI during a short period when the Fe oxy-hydroxides concentrations decrease (**Figures 5**, **6**). However, this release is short-lived, in comparison to the S1 scenario, because MeHg binds onto the newly formed POM (**Figure 5**). Higher concentrations of Hg(II) and MeHg are bioaccumulated in the summer in well-oxygenated systems (S2) than under anoxic conditions in S1 (**Figure 5**). The percentage of Hg_{tot} that is due to dissolved MeHg is 1–2% in the BW and 5% in the upper sediment during summer period,

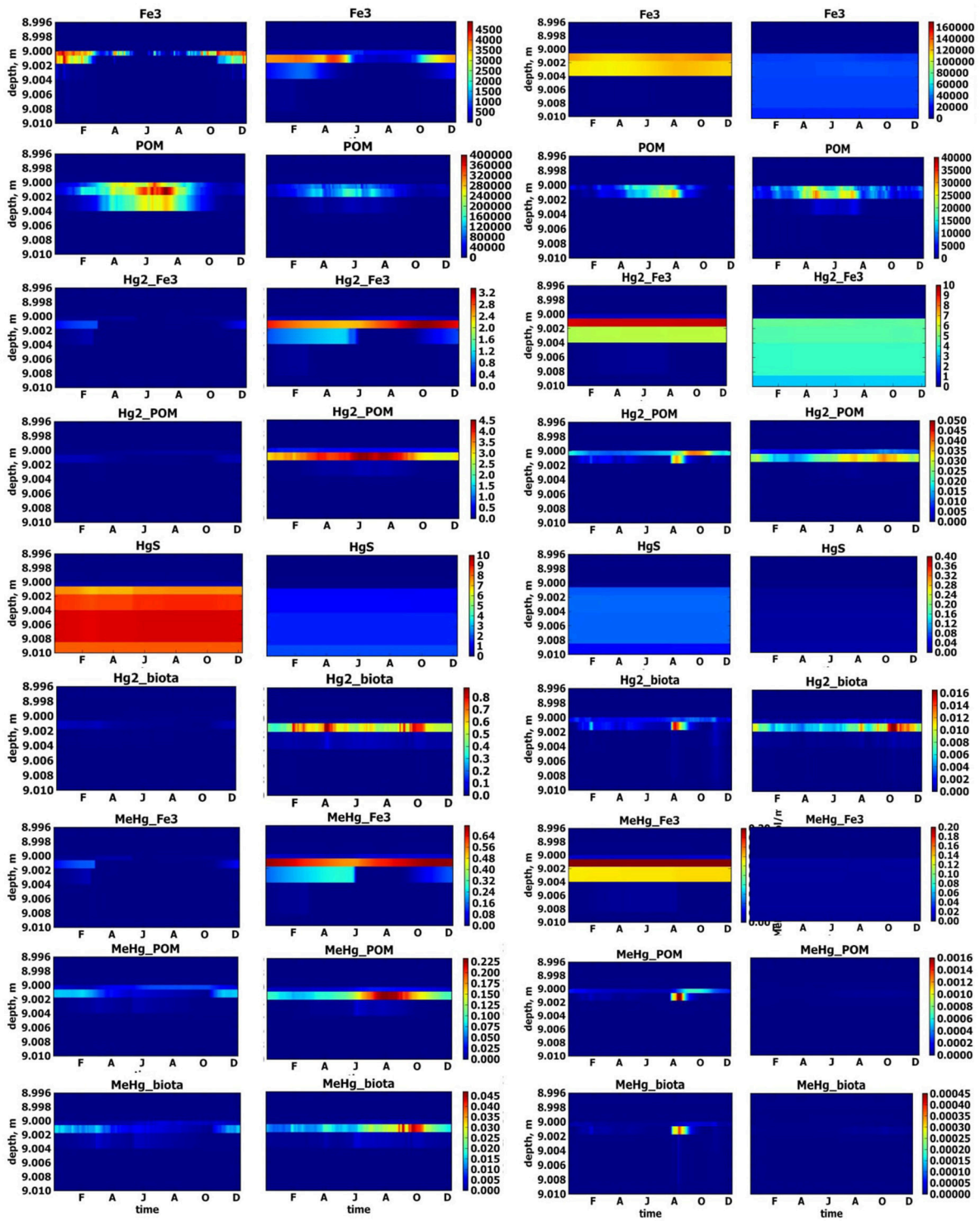

FIGURE 5 | Simulated seasonal dynamic of solid variables (μM) in upper sediment layer for different scenarios, S1–S4. Sediment-water interface is positioned at 9 m depth.

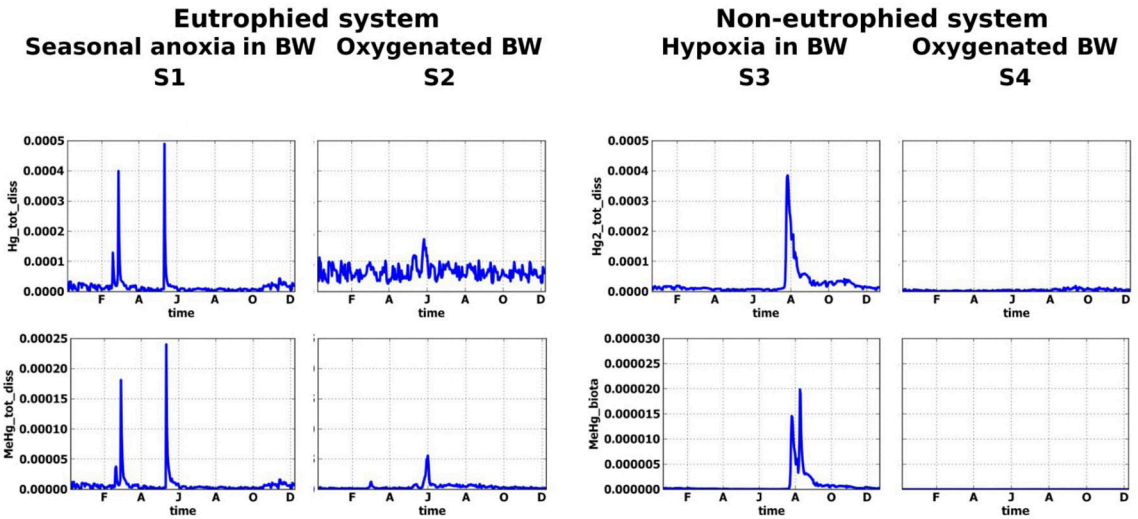

FIGURE 6 | Simulated seasonal dynamic of dissolved Hg(II) and MeHg (μM) at sediment-water interface for different scenarios, S1–S4.

reaching a maximum of 8 and 30% during several days in June.

Influence of the Eutrophication in Well Oxygenated System (S2 vs. S4)

Very low concentrations of hydrogen sulfide (H_2S <6 μM) are found deep in the sediment (>4 cm depth) throughout the year in a well-oxygenated, non-eutrophied system (S4), (**Figure 7**). The content of POM in the upper sediment layer is only about a fifth of the content in a well-oxygenated eutrophied system (S2) due to the lower OM production in a non-eutrophied system (**Figure 5**). Fe oxy-hydroxides are found in the surface sediment throughout the year in both systems, but Fe oxy-hydroxides concentration in surface sediment in S4 is ten times higher than in S2 and they are accumulated in the upper several centimeteres of the sediment (**Figure 5**). The dissolved Hg species concentrations in S4 are several orders of magnitude lower than in S2 (**Figures 6**, **7**). In well-oxygenated, non-eutrophied system, Fe oxy-hydroxides sequesters Hg(II) and bring it to the deeper sediment layer (**Figure 5**). In well-oxygenated, eutrophied systems, OM production/mineralization processes tend to promote the accumulation of Hg and MeHg at the SWI followed by their release to the water and bioaccumulation.

Influence of the Redox Conditions in Non-eutrophied System (S4 vs. S3)

Restricted vertical mixing in a non-eutrophied system (S3) results in seasonal anoxia and the appearance of H_2S in the sediment in concentrations significantly higher than in non-eutrophied system with well oxygenated water (S4) (up to 40 vs. 6 μM, respectively) (**Figure 7**). However, as in S4, H_2S does not appear in the water column in concentration higher 0.1 μM. In S3, the diagenetic processes lead to the accumulation of higher concentrations of Fe oxy-hydroxides in the upper sediment than in the well oxygenated system (**Figure 5**).

When oxic conditions prevail in S3 and S4, Hg(II), and MeHg are accumulated on Fe oxy-hydroxides in the upper sediment layers (**Figure 5**). When reduced conditions occur in S3, relatively high concentrations (with respect to S4) of dissolved Hg and MeHg occur in porewater and the BW during a very short period in August (**Figures 6**, **7**), followed by a decrease in concentrations attributed to the accumulation of Hg species on POM in the sediment. MeHg represented about 1% of total Hg reaching a maximum of 10% in August (**Figures 6**, **7**).

Influence of the Eutrophication in a Low Oxygenated System (S1 vs. S3)

Eutrophication leads to the increased OM formation and accumulation of POM in the sediment. O_2 intensively consumes for decomposition of OM and drops to undetectable levels. The system shifts from hypoxic conditions in the BW to anoxic/sulphidic conditions (**Figure 7**). This causes a higher periodical dissolution of Fe oxy-hydroxides and the release of dissolved Hg species to the BW (**Figures 5**–**7**). High concentrations of sulfide in the porewater binds most of the Hg to insoluble HgS.

In non-eutrophied system Hg species are accumulated on Fe oxides at SWI (**Figure 5**). Shift of redox conditions in the BW from hypoxic to anoxic ($H_2S \sim 0.1$ μM) promotes the release of both Hg(II) and MeHg to the water column (**Figure 7**). Concentration level of these released dissolved Hg species is similar for S1 and S3 (**Figure 6**). The disappearance of oxygen and the establishment of reducing conditions in the BW result in Hg species mobilization both in eutrophied and non-eutrophied systems. But anoxic not sulphidic conditions in BW allows Hg to stay longer in a dissolved form.

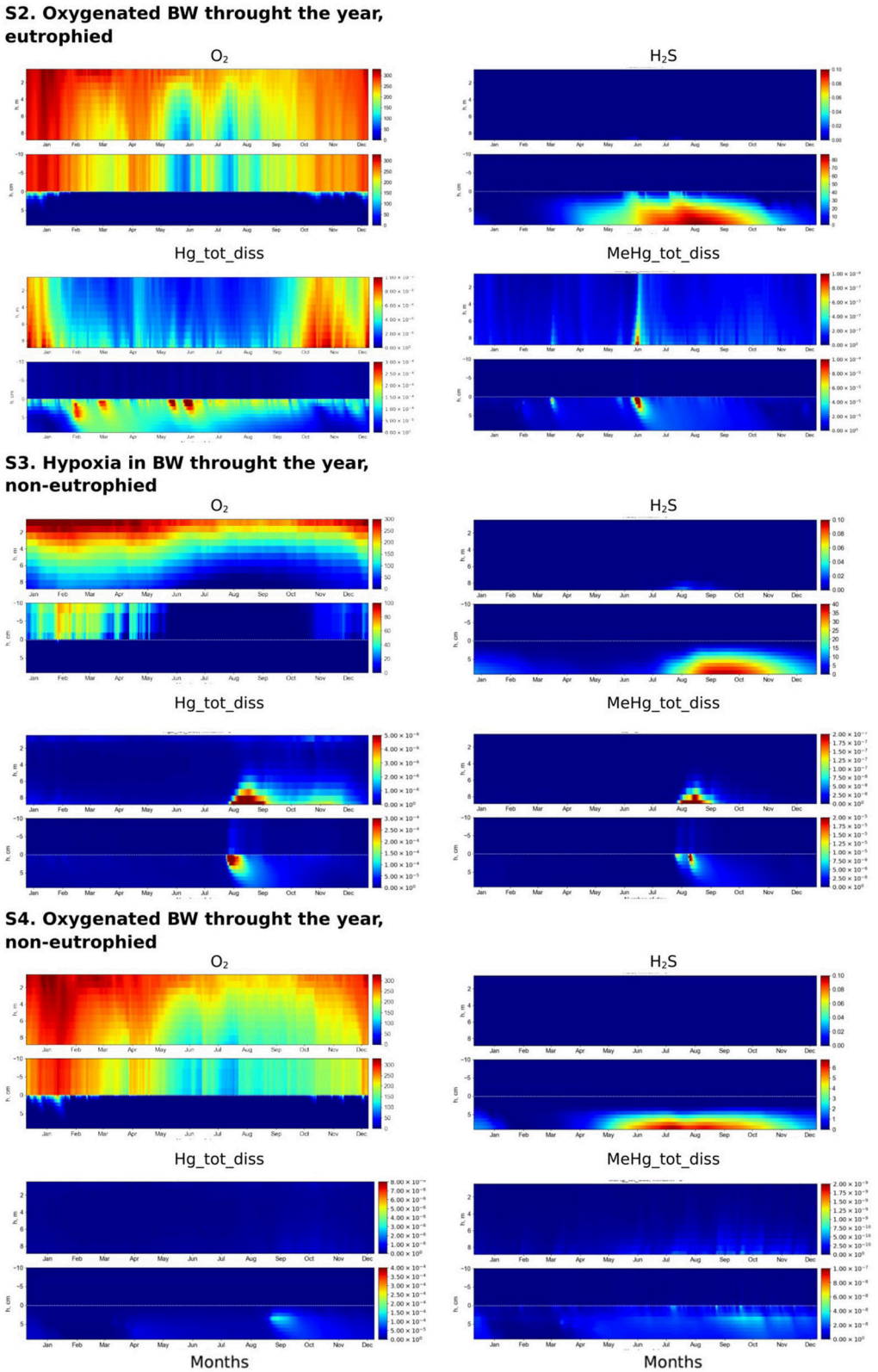

FIGURE 7 | Simulated seasonal dynamics of dissolved oxygen, hydrogen sulfide, total dissolved Hg and MeHg (μM) in the water column and at the sediment-water interface (±10 cm) in the Berre lagoon according to scenarios S2–S4.

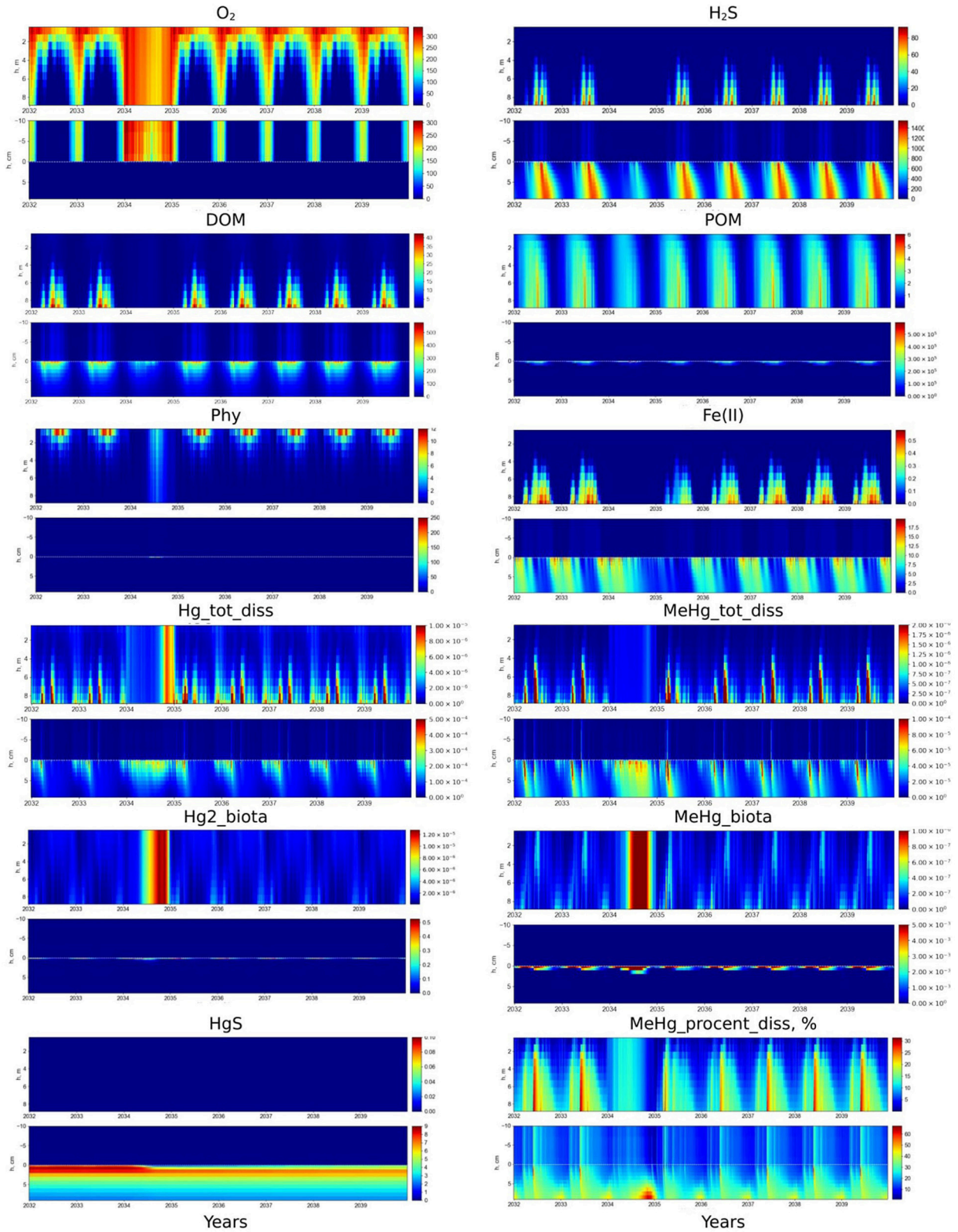

FIGURE 8 | Scenario 5. Seasonal dynamics of dissolved O_2, H_2S, DOM, POM, phytoplankton (Phy), dissolved Fe(II), Hg(II), MeHg, bioaccumulated Hg(II) and MeHg, HgS (μM), and %MeHg in the water column and at the sediment-water interface (±10 cm) in the Berre lagoon. The first 2 years on the figure represent the present state of the lagoon, then 1 year of increased mixing (01.2034 - 12.2034) and then 5 years after the mixing was stopped.

Influence of Both Redox Conditions and Eutrophication on Fate of Hg

Both eutrophication and redox conditions play an important role in Hg cycling, as shown by the results of the simulations. Redox conditions directly control the cycles of some species (i.e., Fe and S) and thus their availability at the SWI. This in turn controls the processes of Hg species sorption and precipitation. Eutrophication partially controls the production of OM, and hence the amount of OM accumulated and degraded in the surface sediment, thereby influencing the redox biogeochemical processes. In addition, production of MeHg is partly dependent on the presence of sulfate reducting bacteria, so its occurrence is favored under reducing conditions at the SWI.

All studied types of sediment, both oxidized and reduced, work as a sink for Hg according to the results of the model. Low concentrations of dissolved Hg species are found in well-oxygenated and non-eutrophied conditions, because they are adsorbed onto the abundant Fe oxides (S4). H_2S formation occurs as a result of eutrophication in reducing conditions in the sediment (S1). The release of H_2S from the sediment to the water column traps Hg species in the particulate phase (as HgS). Afterwards, sulphidic sediments also sequester Hg as HgS.

Therefore, in case of long-term permanent oxic or permanent anoxic conditions in BW and upper sediment, Hg is trapped in the sediments as adsorbed on Fe oxides or as HgS subsequently. In the absence of hydrogen sulfide in the upper sediment, Hg species are accumulated in a thin layer at SWI (S2, S3). Hg immobilization can be expected in all types of the sediments when shift of the redox conditions in BW occurs.

The comparison of studied scenarios allows to conclude that in permanently changing systems, the mobility of Hg at the SWI is expected to be the highest. The simulations of different scenarios show that a well-oxygenated eutrophic system favors the conditions for Hg species bioaccumulation with a potential adverse effect on the ecosystem.

Artificial Lagoon Oxygenation (S5)

Artificial oxygenation by extreme vertical mixing is an option for the management of anoxia in lagoons. We conducted an experiment on the result of S1 by increasing the vertical mixing coefficient by four orders of magnitude during one year, to assess the effect of lagoon oxygenation. Results of the simulation showed that increased vertical mixing fully oxygenated the lagoon and significantly decreased H_2S in the sediment (**Figure 8**). Concentrations of dissolved reduced forms of Fe, Mn and OM all decreased during oxygenation (**Figure 8**). Once extreme mixing ceased, the seasonal dynamics of both O_2 and H_2S returned to their initial state within a year. However, the initial concentrations of Fe, Mn, and OM recovered more slowly, about 3–5 years after the oxygenation event. Sharp growth of autotrophic and heterotrophic communities can be observed in the whole water column and upper sediment under high mixing (**Figure 8**). Results of the simulation of nutrients and redox metals behavior under lagoon oxygenation are in agreement with field experiments of deepwater oxygenation (Stigebrandt et al., 2015).

Concentrations of dissolved Hg(II) and MeHg increase in the porewaters during the period of oxygenation (**Figure 8**). The upper sediment is oxygenated after several months of increased mixing which favors the dissolution of Hg sulfide, thereby rapidly increasing and maintaining a high Hg(II) concentration in the BW. In addition, the faster degradation of OM under oxic conditions also favors the release of Hg to the BW. Intensive vertical mixing brings all the Hg forms from the BW up to the surface waters, so bioaccumulation processes can take place throughout the water column.

Nevertheless, the average concentration of MeHg (0.6 pM) in the water column during the ventilation remains lower than in BW during the seasonal appearance of anoxia in the lagoon (10-20 pM) (**Figure 8**). In the case of water oxygenation, MeHg is released to the water and rapidly bioaccumulated by autotrophic and heterotrophic organisms in the whole water column (**Figure 8**). The concentration of dissolved MeHg, the amount of MeHg% and bioaccumulated MeHg in the water column decrease at the end of period of high mixing (**Figure 8**). The dissolved MeHg is adsorbed on Fe oxides (MeHg_Fe3 increases) and returns to the sediment. The amount of Hg(II) adsorbed on Fe oxides also increased at the end of ventilation, however most of the Hg(II) remains in the water column. Once the ventilation stops, it takes about 3 years for the seasonal dynamics of Hg species re-establish.

Episodic oxygenation events in eutrophied and sulphidic environments can have a negative effect on the ecosystem (Sternbeck et al., 1999, Pakhomova et al., 2014). The model results both confirm and explain the possible mechanisms of this effect. The rate of many Hg transformations, including Hg sulfide oxidation rate, depends on the presence of different type of OM in the sediment (Ravichandran et al., 1998). New data of the temporal trend of Hg species are needed to improve the calculation. A decreasing occurrence of hypoxia allows the recolonization of sediment by benthic organisms that may impact the biogeochemical cycle of Hg and its transport through the SWI (Benoit et al., 2009). The role of benthic fauna bioturbation activity may thus have to be evaluated with specifically collected data, in order to comprehend their influence on the fate of mercury in the Berre lagoon.

The simulation of the lagoon oxygenation under increased vertical mixing (S5) predicts a mobilization of Hg from the sediment, resulting in a period of increased content of dissolved Hg species in the whole water column, followed by trapping of Hg species back into the sediment. Therefore, such management measures can increase the risk associated to the entering of Hg to the food chain. Simulations of different scenarios of the lagoon oxygenation using BROM can be useful to find the optimal conditions for water mixing with minimum negative effect on the ecosystem.

CONCLUSIONS

An Hg biogeochemical transformation module was developed and added to BROM, a coupled benthic-pelagic reactive-transport model. The modified BROM was used to simulate

five case scenarios in the Berre lagoon. The aim was to study the fate of Hg in the water column and upper sediment layer under different conditions. The scenarios consider eutrophied and non-eutrophied systems under well oxygenated, hypoxic and seasonally anoxic conditions in bottom water, and artificial oxygenation of the lagoon.

Simulation results showed that both oxidized and reduced sediments can accumulate Hg, but any shifts in redox conditions in bottom water and upper sediment layer lead to the release of Hg species into the water column. Iron oxides are the main sources of Hg immobilization in case of oxic sediments in non-eutrophied system while particulate organic matter plays an important role for Hg dynamics in well oxygenated eutrophied system. For the sulfidic sediment, the main source of mercury immobilization is Hg sulfide. Eutrophication or/and restricted vertical mixing lead to intensive MeHg formation in the sediment and its possible subsequent release to the water. Long- term stable redox conditions in the bottom water allow Hg species to be accumulated in the upper sediment layer. The model predicts that the highest benthic flux of Hg species into the bottom water can occur when there is a sharp shift of redox conditions after a long period of stable oxic or anoxic conditions. Oxygenation of an anoxic water body leads to the appearance of Hg species in the water column and the potential bioaccumulation by living organisms. This way may be the main route of Hg to biota and presents an associated contamination risk for the aquatic ecosystem.

Simulation results of spatial and temporal distributions of studied parameters under different conditions showed good agreements with the field data. BROM may thus be used to predict the fate of Hg trapped in sediment for different management scenarios.

AUTHOR CONTRIBUTIONS

SP leaded the paper writing and mercury model processes parameterization; EY leaded the work on model development and wrote the paper; EP worked on the model code, performed the work on github and contributed to the paper; SR, DC, JK, and OR participated in the field studies and wrote the paper; SY was responsible for the model code development; DK contributed to the code development and wrote the paper; R-MC and AN contributed to the results discussion and wrote the paper.

FUNDING

The contribution of SP was funded by VISTA — a basic research program and collaborative partnership between the Norwegian Academy of Science and Letters and Statoil, project no. 6164. R-MC, EY, and DK were funded by the project PREDHYPO, carried out thanks to the support of the A*MIDEX project (no. ANR-11-IDEX-0001-02) funded by the Investissements d'Avenir French Government program, managed by the French National Research Agency (ANR). The contributions of EP, and EY were supported by the Norwegian Research Council SKATTEfunn project 272749 Aquatic Modeling Tools. Alice Newton acknowledges the support of NILU, CIMA, IMBER, Future Earth Coasts, and Future Earth Ocean KAN.

REFERENCES

Allison, J., and Allison, T. (2005). *Partition Coefficients for Metals in Surface Water, Soil, and Waste*, Washington, DC: USEPA

Barber, M. C., Suárez, L. A., and Lassiter, R. R. (1991). Modelling bioaccumulation of organic pollutants in fish with an application to PCBs in lake *Ontario Salmonids*. *Can. J. Fish. Aquat. Sci.* 48, 318–337 doi: 10.1139/f91-044

Benoit, J. M., Shull, D. H., Harvey, R. M., and Beal, S. A. (2009). Effect of bioirrigation on sediment-water exchange of methylmercury in Boston Harbor, Massachusetts. *Environ. Sci. Technol.* 43, 3669–3674. doi: 10.1021/es803552q

Bigham, G. N., Murray, K. J., Masue-Slowey, Y., and Henry, E. A. (2016). Biogeochemical controls on MeHg in soils and sediments: implications for site management. *Integr. Environ. Assess. Manage.* 13, 249–263. doi: 10.1002/ieam.1822

Bruggeman, J., and Bolding, K. (2014). A general framework for aquatic biogeochemical models. *Environ. Model. Softw.* 61:249–265. doi: 10.1016/j.envsoft.2014.04.002

Canu, D., Acquavita, A., Knightes, C. D., Mattassi, G., Scroccaro, I., and Solidoro, C. (2012). "Modeling the mercury cycle in the marano-grado lagoon (Italy)," in *Book: Models of the Ecological Hierarchy*, Developments in Environmental Modelling, eds F. Jordan and S. E. Jorgensen (Amsterdam; Oxford: Elsevier), 25.

Chakraborty, P., Sarkar, A., Vudamala, K., Naik, R., and Nath, B. N. (2015). Organic matter — a key factor in controlling mercury distribution in estuarine sediment. *Mar. Chem.* 173, 302–309. doi: 10.1016/j.marchem.2014.10.005

Cossa, D., Garnier, C., Buscail, R., Elbaz-Poulichet, R., Mikac, N., Patel-Sorrentino, N., et al. (2014). A Michaelis-Menten type equation for describing MeHg dependence on inorganic mercury in aquatic sediments. *Biogeochemistry* 119, 35–43. doi: 10.1007/s10533-013-9924-3

Covelli, S., Faganeli, J., Horvat, M., and Brambati, A. (1999). Porewater distribution and benthic flux measurements of mercury and methylmercury in the Gulf of Trieste (northern Adriatic Sea). *Estuar. Coast Shelf Sci.* 48, 415–428.

Driscoll, C. T., Mason, R. P., Chan, H. M., Jacob, D. J., and Pirrone, N. (2013). Mercury as a global pollutant: sources, pathways, and effects. *Environ. Sci. Technol.* 47, 4967–4983. doi: 10.1021/es305071v

EC (2000). *Directive 2000/60/EC of the European Parliament and of the Council of 23 October 2000 Establishing a Framework for Community Action in the Field of Water Policy*. OJ L 327, 22.12.2000.

EC (2008). *Directive 2008/105/EC of the European Parliament and of the Council of 16 December 2008 on Environmental Quality Standards in the Field of Water Policy, Amending and Subsequently Repealing Council Directives 82/176/EEC, 83/513/EEC, 84/156/EEC, 84/491/EEC, 86/280/EEC and amending Directive 2000/60/EC of the European Parliament and of the Council*. OJ L 348, 24.12.2008

EC (2017). Regulation (EU) 2017/852 of the European Parliament and of the Council of 17 May 2017 on mercury, and repealing Regulation (EC) No 1102/2008 OJ L 137, 24.5.2017

Fitzgerald, W. F., and Clarkson, T. W. (1991). Mercury and monoMeHg: present and future concerns. *Environ. Health Perspect.* 96, 159–166. doi: 10.1289/ehp.9196159

Fitzgerald, W. F., Lamborg, C. H., and Hammerschmidt, C. R. (2007) Marine biogeochemical cycling of mercury. *Chemical Rev.* 107, 641–662. doi: 10.1021/cr050353m

Gargett, A. E. (1984). Vertical eddy diffusivity in the ocean interior. *J. Mar. Res.* 42, 359–393.

Jeliazovski, F., Lux M., and Penard, C. (2015). *Modelisation Hydrodynamique de l'etang de Berre et des Millieux Annexes*. Labege: Noveltis.

Jeong, H. Y., Sun, K., and Hayes, K. F. (2010). Microscopic and spectroscopic characterization of Hg(II) immobilization by mackinawite (FeS). *Environ. Sci. Technol.* 44, 7476–7483 doi: 10.1021/es100808y

Katsev, S., Tsandev, I., L'Heureux, I., and Rancourt, D. G. (2006). Factors controlling long-term phosphorus efflux from lake sediments: exploratory reactive-transport modeling. *Chem. Geol.* 234, 127–147. doi: 10.1016/j.chemgeo.2006.05.001

Knightes, C. D. (2008). Development and test application of a screening-level mercury fate model and tool for evaluating wildlife exposure risk for surface waters with mercury- contaminated sediments (SERAFM). *Environ Model Softw.* 23, 495–510. doi: 10.1016/j.envsoft.2007.07.002

Kudo, A. (1992). Natural and artificial mercury decontamination - Ottawa River and Minamata Bay (Yatsushiro Sea). *Water Sci. Technol.* 26, 217–226. doi: 10.2166/wst.1992.0402

Liu, G., Cai, Y., O'Driscoll, N., Feng, X., and Jiang, G. (2012). "Overview of mercury in the environment," in *Environmental Chemistry and Toxicology of Mercury,* eds G. Liu, Y. Cai, and N. O'Driscoll (New York, NY: John Wiley and Sons, Inc).

Mackay, D. (2001). *Multimedia Environmental Models: The Fugacity Approach.* Boca Raton, FL: CRC Press.

Massoudieh, A., Bombardelli, F. A., and Ginn, T. R. (2010). A biogeochemical model of contaminant fate and transport in river waters and sediments. *J. Contam. Hydrol.* 112, 103–117. doi: 10.1016/j.jconhyd.2009.11.001

O'Higgins, T., Tett, P., Farmer, A., Cooper, P., Dolch, T., Friedrich, J., et al. (2014). Temporal constraints on ecosystem management: definitions and examples from Europe's regional seas. *Ecol. Soc.* 19:46. doi: 10.5751/ES-06507-190446

Pakhomova, S., Braaten, H. F. V., Yakushev, E., and Skei, J. (2014). Positive and negative biogeochemical effects following an oxygenated intrusion into anoxic fjord system. *Geochem. Trans.* 15:5. doi: 10.1186/1467-4866-15-5

Ravichandran, M., Aiken, G. R., Reddy, M. M., and Ryan, J. N. (1998). Enhanced dissolution of cinnabar (Mercuric Sulfide) by dissolved organic matter isolated from the Florida Everglades. *Environ. Sci. Technol.* 32, 3305–3311 doi: 10.1021/es9804058

Rigaud, S., Radakovitch, O., Couture, R. M., Deflandre, B., Cossa, D., et al. (2013). Mobility and fluxes of trace elements and nutrients at the sediment–water interface of a lagoon under contrasting water column oxygenation conditions. *Appl. Geochem.* 31, 35–51. doi: 10.1016/j.apgeochem.2012.12.003

Rigaud, S., Radakovitch, O., Nerini, D., Picon, P., and Garnier, J. M. (2011). Reconstructing historical trends of Berre lagoon contamination from surface sediment datasets: influences of industrial regulations and anthropogenic silt inputs. *J. Environ. Manage.* 92, 2201–2210. doi: 10.1016/j.jenvman.2011.04.002

Sternbeck, J., Skei, J., Verta, M., and Østlund, P. (1999). Mobilisation of sedimentary trace metals following improved oxygen conditions: an assessment of the impact of a lowered primary productivity on trace metal cycling in the marine environment. *TemaNord* 594:65

Stigebrandt, A., Liljebladh, B., de Brabandere, L., Forth, M., Granmo, Å., Hall, P., et al. (2015). An experiment with forced oxygenation of the deepwater of the anoxic by Fjord, Western Sweden. *Ambio.* 44, 42–54. doi: 10.1007/s13280-014-0524-9

Tseng, C. M., de Diego, A., Pinaly, H., Amouroux, D., and Donard, O. F. X. (1998). Cryofocusing coupled to atomic absorption spectrometry for rapid and simple mercury speciation in environmental matrices. *J. Anal. At. Spectrom.* 13, 755–764.

United Nations (2017). *Minimata Convention on Mercury*. Nairobi.

Wang, Q., Kim D., Dionysiou D. D., Sorial G. A., Timberlake D. (2004). Sources and remediation for mercury contamination in aquatic systemsda literature review. *Environ. Pollut.* 131, 323–336. doi: 10.1016/j.envpol.2004.01.010

Waples, J. S., Nagy, K. L., Aiken, G. R., and Ryan, J. N. (2005). Dissolution of cinnabar (HgS) in the presence of natural organic matter. *Cheochim cosmochim acta* 69, 1575–1588. doi: 10.1016/j.gca.2004.09.029

Yakushev, E., Protsenko, E., Bruggeman, J., Wallhead, P., Pakhomova, S., Yakubov, S., et al. (2017). Bottom RedOx Model (BROM v.1.1): a coupled benthic–pelagic model for simulation of water and sediment biogeochemistry. *Geosci. Model Dev.* 10, 453–482. doi: 10.5194/gmd-10-453-2017

Conflict of Interest Statement: The authors declare that the research was conducted in the absence of any commercial or financial relationships that could be construed as a potential conflict of interest.